ADVANCED FUNCTIONAL MATERIALS
www.afm-journal.de

A Biomimetic Drosera Capensis with Adaptive Decision-Predation Behavior Based on Multifunctional Sensing and Fast Actuating Capability

Ye Qiu, Chengjun Wang, Xiaoyan Lu, Huaping Wu, Xiaolong Ma, Jiahui Hu, Hangcheng Qi, Ye Tian, Zheng Zhang, Guanjun Bao, Hao Chai, Jizhou Song,* and Aiping Liu**

The sophistication, adaptability, and complexity of biological systems have provided enormous inspiration and have been a continuous source of numerous innovations. Soft living organisms like drosera capensis have amazing predatory behavior that can capture prey of ideal size, enabling them to interact with environmental stimuli efficiently. Mimicking such natural intelligence in artificial systems with systematical functions of multiple information perception, neuronal transmission, and adaptive motility remains a grand challenge. Here, a biomimetic drosera capensis is reported that is capable of multifunctional self-sensing, automatic regulation, and adaptive actuation in response to diverse stimuli with intelligent predation capability in an entirely closed-loop fashion. The functional system heterogeneously integrates the thermal-responsive soft actuator as the muscle-like motor and flexible tactile, strain, and piezoelectric multimodal sensors as somatosensory receptors. With the synergistic effect of multifunctional sensing and fast actuating schemes, the artificial drosera capensis deconvolutes multiple characteristics of the catching process (e.g., strain rate, magnitude, and direction) and thus holds impressive predatory behavior for ideal-sized prey. This electronically innervated artificial drosera capensis with multimodal sensing and self-regulated actuating capability through the closed-loop control of sensing and actuating system paves the way for the development of adaptive soft robots.

1. Introduction

Biological systems are sophisticated engineers that have evolved vast delicate and versatile regulating mechanisms for efficiently adapting to environmental changes, which offers fertile inspiration for the design of intelligent robots.[1–4] Many living organisms in nature are capable of self-perception and autonomous response to a variety of surrounding stimuli and show a fascinating adaptative control strategy via the feedback from their epidermal sensory cells.[5] Of particular interest, carnivorous plant drosera capensis can automatically fold its leaves to digest small insects (e.g., mosquitos and flies) trapped on its surface (**Figure 1**A) and release large prey like moths and butterflies.[6] The rapid response to external stimuli and the amazing capability of behavior regulation arouse a large amount of bionic inventions aiming at autonomous perception feedback.[7–9] However, to mimic the complicated biological sensory

Y. Qiu, H. Wu, X. Ma, J. Hu, H. Qi, Y. Tian, Z. Zhang, G. Bao
College of Mechanical Engineering
Zhejiang University of Technology
Hangzhou 310023, China
E-mail: hpwu@zjut.edu.cn, wuhuaping@gmail.com

Y. Qiu, H. Wu, X. Ma, J. Hu, H. Qi, Y. Tian, Z. Zhang, G. Bao
Key Laboratory of Special Purpose Equipment and Advanced Processing Technology
Ministry of Education and Zhejiang Province
Zhejiang University of Technology
Hangzhou 310023, China

C. Wang, J. Song
Department of Engineering Mechanics
Soft Matter Research Center and Key Laboratory of Soft Machines and Smart Devices of Zhejiang Province
Zhejiang University
Hangzhou 310027, China
E-mail: jzsong@zju.edu.cn

X. Lu
School of Civil Engineering
Harbin Institute of Technology
Harbin 150001, China

H. Wu
Collaborative Innovation Center of High-end Laser Manufacturing Equipment (National "2011 Plan")
Zhejiang University of Technology
Hangzhou 310014, China

H. Chai
Department of Engineering Mechanics
Zhijiang College of Zhejiang University of Technology
Shaoxing 312030, China

A. Liu
Center for Optoelectronics Materials and Devices
Zhejiang Sci-Tech University
Hangzhou 310018, China
E-mail: liuap@zstu.edu.cn, liuaiping1979@gmail.com

The ORCID identification number(s) for the author(s) of this article can be found under https://doi.org/10.1002/adfm.202110296.

DOI: 10.1002/adfm.202110296

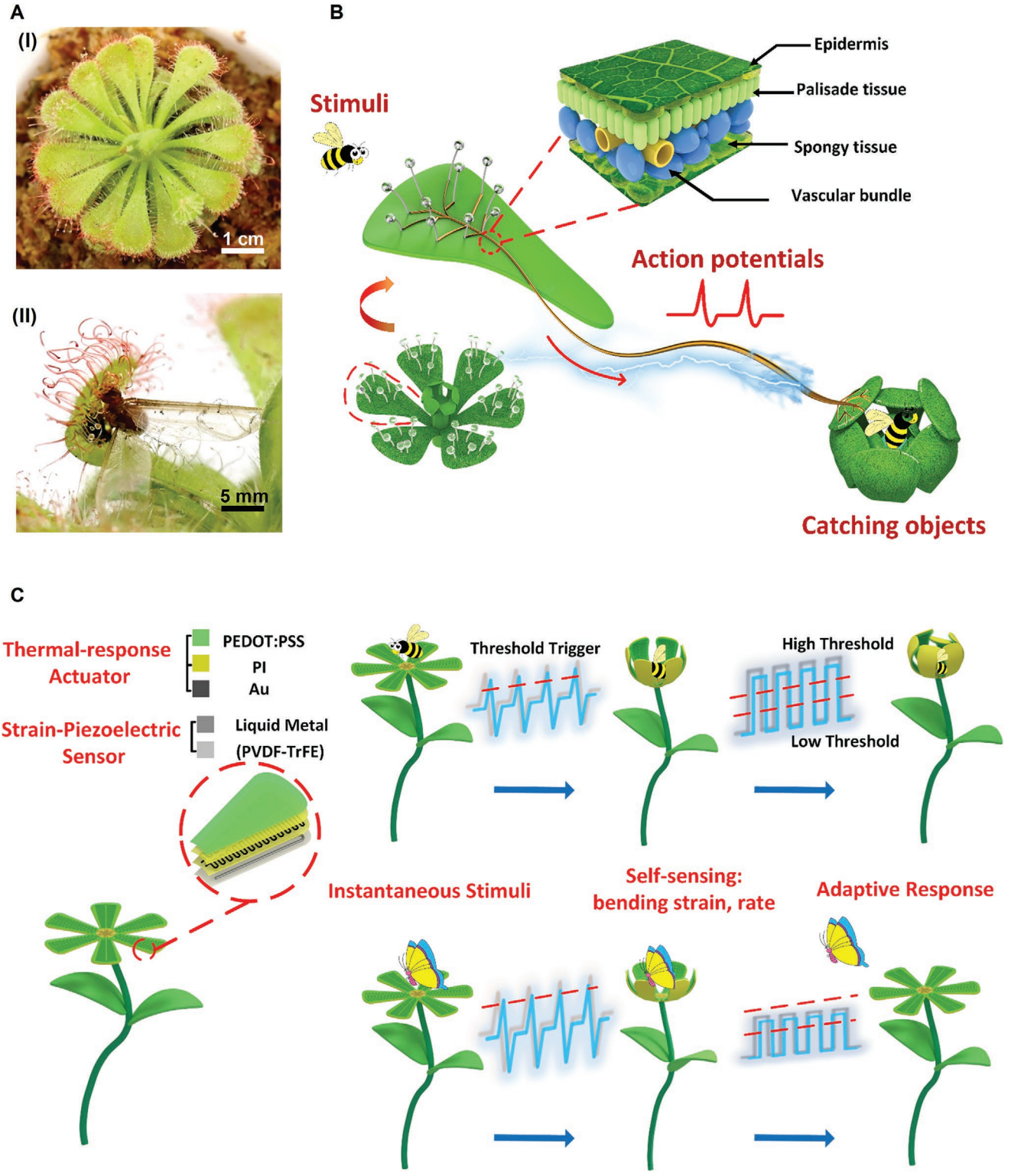

Figure 1. A biomimetic electronic drosera capensis with intelligent predation capability. A) Photograph of a drosera capensis at its (I) open stage, and (II) close upon the stimulation of prey. B) The working mechanism of a drosera capensis when catching the prey. C) Schematic illustrations of the structure of the biomimetic electronic drosera capensis composed of soft actuator and flexible multimodal sensors: the piezoelectric tactile sensor mimics the action potential induced by the stimulus of the drosera capensis to sense the instantaneous stimuli, which further converts the mechanical stimuli to electrical signals to trigger the rapid closure of the soft actuator. The self-sensing bending strain and strain rate information through the strain and piezoelectric sensors are further applied to the actuator to induce self-regulated and feedback-type actuation to smartly catch the small preys and release the large preys.

function and fully adaptive actuation in artificial systems remains a daunting challenge, which requires an accumulative understanding of biology and the manufacturing technology of artificial stimuli-responsive motility integrated with both sensing and actuating capability.

Recent advances in flexible electronics and soft actuators have bridged the gap between robots and living organisms and paved the way for creating intelligent soft robots,[3,4,7–13] human-machine interfaces,[14–16] and electronic prostheses.[17,18] Soft robots inspired by soft organisms like octopus, inchworm, and flytrap are designed with diverse actuation strategies (e.g., electrical, light, humidity, pneumatic, and magnetic actuation), which can perform complex deformability with agile and easy operation.[1–4,8–11,19–23] To realize real-time motion feedback and interact with the surrounding environment, intelligent soft robots integrated with somatosensory functionality have also been explored.[3,7,11,24–30] Multiple embodiments emerged with several single modes of sensory feedback mechanisms, such as ionic capacitive sensors,[31] piezoresistive strain sensors,[32] and triboelectric robotic skins[26] can efficiently perceive their muscle motions for further action. Meanwhile, the developed systematical functions of signal sensing and processing technology have been incorporated into the robot system and further reinforce the capability of sensing and responding to external stimuli.[3,29,30] However, it is still a challenge to achieve trade-offs of fast actuating and multiple self-sensing capabilities with the separated sensing and responding functional module, and heavily limit their applications in human-machine interfaces and robot-environment interactions where autonomous perceptual feedback and adaptive motor responses are desired to work synergetically.

Inspired by the physiological functions and unique predation capability of drosera capensis, we here demonstrate a biomimetic electronic drosera capensis that is capable of autonomously recognizing and adaptively capturing prey of ideal size through a closed-loop actuation and multimodal sensing system (Figure 1C). Trade-offs of the functional system between the fast actuating and multiple self-sensing capabilities are achieved by utilizing structural design, device fabrication, and functional integration. The piezoelectric tactile sensor mimics the action potential of the drosera capensis with the sense of instantaneous stimuli, then the mechanical stimuli induced electrical signals were recognized to further trigger the rapid bending of the soft actuator. The bending strain, strain rate, and bending direction of the soft actuator can be autonomously recognized through a self-regulated feedback system, which is further utilized to capture small prey and release large prey for self-protection. The artificial drosera capensis assisted with multimodal sensory feedback (i.e., tactile, strain, and strain rate) and programmable soft actuators can have fast and adaptive predatory behavior just like drosera capensis does. This self-regulated actuation ability in response to the diverse stimulation opens up avenues towards soft, autonomous bio-inspired soft robots.

2. Results and Discussion

2.1. Programmable Soft Actuator for Biomimetic Drosera Capensis

The ability of prey selectivity of drosera capensis lies in the unique biological system, where the sensory receptor (i.e., glandular hairs) transmits action potentials from the partial epidermis to the whole leaves through the vascular bundle (Figure 1B), thereby leading to the secretion of auxin (i.e., jasmonates) to trigger predatory behavior.[33,34] The secret is the asymmetric auxin distribution in upper and lower epidermal cells in the leaves leading to a bending motion of cellular architecture stimulated by a simple isotropic biochemical signal.[35] Such a predation mechanism enables the drosera capensis response rapidly to interact with surrounding environments and distinguish various stimuli for self-regulation via autonomous motility and perception feedback system.

To mimic the fast predation behavior (<10 s) of drosera capensis, a thermal-responsive soft actuator embedded with a programmable flexible heater was developed as the artificial muscle of the biomimetic drosera capensis. The soft actuator is composed of an active thermal-responsive and a passive thermal-inert bilayer, which converts the strain mismatch under the joule heat into a reversible bending deformation (**Figure 2**A). The shrinking strain of thermal-responsive poly(3,4-ethylenedioxythiophene): polystyrene sulfonate (PEDOT: PSS) layer can increase up to 6% as the temperature increases from 25 to 100 °C, while the thermal expansion of thermal-inert polyimide (PI) layer is only 0.01%.[36,37] With this thermal-inert/responsive hetero-deformation bilayer, bending motion can be realized after the applied actuation voltage, as demonstrated in optical images with a bilayer size of 2 cm × 1 cm (Figure 2B,C).

The temperature increase rate and distribution of bilayer morphing structure significantly affect the bending behavior. The heating performance of the flexible heater can be evaluated quantitatively by connecting a flexible anisotropic conductive film cable through the contact pads to deliver currents. The temperature can increase rapidly within 5 s and drop quickly to the initial state over the current range from 10 to 30 mA (Figure 2D), indicating the efficiency of the embedded flexible heater to drive the actuator. The resistance of the heater in Figure 2D is 260 Ω, the driving voltages corresponding to the 10, 20, and 30 mA current are 2.6, 5.2, and 7.8 V, respectively. The temperature distribution and curvature change of the bilayer morphing structure can be further predicted by a thermo-mechanical analytical model, as described in the Supplementary Materials. Results show well-behaved, linear variations of temperature with respect to applied current (Figure 2E and Figure S1, Supporting Information), which further leads to a linear curvature variation due to the bimorph structure. The bending curvature of the actuator can reach to 1.6 cm^{-1} with a heating temperature of 90 °C within 5 s, which agrees reasonably well with results from finite element analyses and experimental observations (Figure 2F). Compared to bilayer morphing actuators in literatures (Table S1, Supporting Information), this flexible actuator exhibits superior actuating behavior[38–42] including large bending curvature (1.67 cm^{-1}), fast response (5 s), and recover time (7 s) with a relatively low heating temperature (90 °C) (Figure 2G). This remarkable acting behavior benefits from the significant difference in thermal response between PEDOT: PSS and PI of the ultrathin bimorph structure. The excellent bend-and-release performance has good reversibility and reliability repeated without a decrease in bending curvature (Figure 2H) after periodic circles.

To mimic the geometric shape and predation behavior of the drosera capensis, the soft actuator with six petals was created

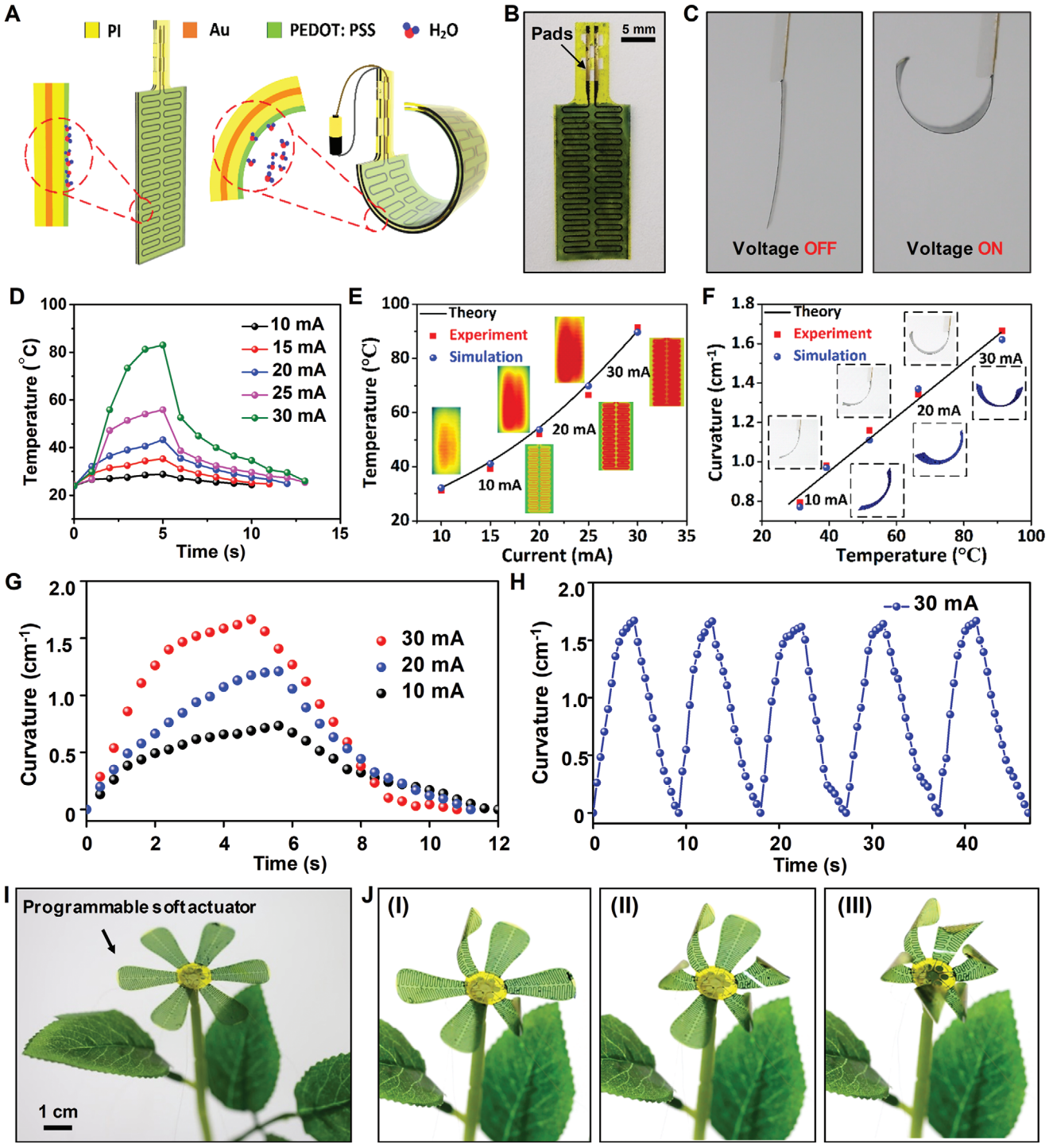

Figure 2. Drosera capensis-inspired programmable soft actuator. A) The actuating mechanism of the programmable soft actuator by an imbedded flexible heater. B) Optical images of the fabricated soft actuator C) before and after applying the voltage. D) The temperature distributions at the top surface of the heater under various applied currents as a function of time. A comparison of E) temperature distributions at the top surface of the heater and F) bending curvatures of the soft actuator between the theoretical predictions, simulation results, and experimental demonstrations. G) The bending curvature of the soft actuator for the applied current from 10 to 30 mA. H) The cycled deformation of the soft actuator under 30 mA current. I) Optical images of the flytrap-inspired soft actuator with independent addressable capability and J) its sequence bending deformation in a programmable manner.

and fixed on the plastic branch. The design of vein-shaped and serpentine layout distributed heaters is introduced into a soft structure to generate uniform and enough joule heat (Figure S2, Supporting Information). Each petal can be independently controlled in a programmable manner (Figure 2I). With the independently distributed heater, arbitrary configurations can

be assembled with addressable capability on demand. Therefore, the shapes of the flower-like soft actuator can be digitally manipulated. Sequential actuation of each addressable petal, as an example, is shown in Figure 2J. All petals exhibit rapid and controllable bending deformation, showing repetitive closure and unfolding behaviors like a real drosera capensis in nature to capture the prey (Movie S1, Supporting Information).

2.2. Multimodal Sensory for Biomimetic Drosera Capensis

The complicated biological sensory cells distributed on the epidermis of living organisms play critical roles for them to adapt to surrounding stimuli via the sensing feedback control. The self-sensing capability of predatory behavior of the biomimetic drosera capensis includes the instantaneous impact of prey and real-time deformation of petals, which requires a multifunctional self-sensing capability to respond to dynamic and static stimuli simultaneously. To mimic the sensory function of the drosera capensis, the integrated sensory design comprises two sensing mechanisms (i.e., piezoelectric and piezoresistive) to simultaneously detect static and dynamic mechanical stimuli over the predation process. Specifically, flexible multimodal sensors including strain sensors (patterned liquid metal (LM) wires, gallium-based alloy)[43–45] and piezoelectric sensors polyvinylidene fluoride-trifluoroethylene (P(VDF-TrFE)) are created and integrated with the soft actuator (**Figure 3**A, 3B, and Figure S3, Supporting Information). The captured sensing information will be further programmed and give feedback to the actuators for this self-regulated system in the predation process.

Multifunctional sensing systems mainly suffer from the inherent limitations in the simple combination of the measured stimuli, without further exploration of the sensing capability to realize the synergistic effect of sensing modes. To overcome this challenge, a comprehensive analysis of the measured signals is investigated to extend the full potential of sensing systems. The strain and strain rate captured by the integrated multimodal sensors provide real-time voltage applied on the soft actuator. The above mentioned 1.67 cm^{-1} bending curvature under 30 mA current can be immediately sensed by the liquid metal wires with a resistance change of about 18% (Figure 3C), showing the excellent capability of the bending strain detection (Figure 3D). Temperature effect on the liquid metal is only 7% of the total relative resistance change, which is negligible (Figure S4, Supporting Information). Meanwhile, the capability of the piezoelectric mode to detect the strain rate (Figure 3E) relies on its frequency-dependent response,[46] indicating that various loading rates of the stimuli can lead to the discrepancy of the piezoelectric voltage. The deformation rate ranged from 0.15 to 0.42 cm^{-1} s^{-1} can be precisely detected through the increased peak value of piezoelectric voltage (Figure 3F), which is well-suited to detect the bending speed of the soft actuator.

Simultaneous measurements of piezoelectric and strain signals from the actuating process are tested to validate their applications toward multifunctional sensing capabilities. The synergistic effect of the strain and piezoelectric modes' responses to stimuli allow further decoding of the real-time deformation of the actuator (Figure 3G,H). For instance, the increase in the relative change of resistance from zero together with two positive piezoelectric pulses indicates two positive bending deformation processes. Following a bending curvature rate of 0.24 and 0.27 cm^{-1} s^{-1}, the bending curvature of the soft actuator increases to 1.2 cm^{-1} and then to 1.8 cm^{-1} during the two positive bending steps. Next, the decrease in the relative change of resistance to zero together with two negative piezoelectric pulses indicates two reverse recovering processes to reduce the bending curvature down to zero at a bending curvature rate of 0.23 and 0.21 cm^{-1} s^{-1}, respectively. Consequently, the bending strain, strain rate, and direction of the soft actuator during bending deformation can be perceived by the synergistic effect of piezoresistive and piezoelectric sensors. Therefore, the results indicate that an attractive feature of the integrated sensing layers is the multifunctional sensing functionality, especially for the unique capability to capture the whole predation process. Precisely capturing the real-time deformation process of the actuator provides a design concept for meeting the challenges in the realization of multiple information synchronous perception, which creates application opportunities for intelligent soft robots in self-sensing feedback and further control.

2.3. Biomimetic Drosera Capensis with Intelligent Predation Capability

As a proof-of-concept demonstration, the artificial bionic drosera capensis that consists of the independent addressable, programmable soft actuator and the multimodal sensors is created and connected to the external circuit to achieve the intelligent predation process, as the drosera capensis in nature does. The special piezoelectric P(VDF-TrFE) based tactile sensor integrated on the center of the soft actuator exhibits an excellent capability to detect the pressure signal (Figure S5, Supporting Information). Evaluation of the fabricated flexible piezoelectric sensor reveals the minimum detectable pressure of 100 Pa for the piezoelectric mode to trigger the actuating deformation (Figure S5A, Supporting Information). The adaptive control circuit of the intelligent predation process is programmed on the Arduino NANO development board with the analog-to-digital conversion module (AD620, ADS1115) and the 2-way 5 V relay module (Figures S6 and S7, Supporting Information), as described in the Supplementary Materials. To demonstrate the intelligent predation capability of biomimetic drosera capensis, the smart manipulator is integrated into a robot arm to execute the dexterous manipulation of releasing objects as instructed by the micro-controller (Movies S2 and S3, Supporting Information). When the biomimetic drosera capensis suffers from a transient external stimulus (i.e., 250 Pa, **Figure 4**A-i), the pressure signal detected by the piezoelectric tactile sensor will be judged. Once the pressure signal is large enough and beyond the threshold of 10 mV (Figure 4A-ii), the electronic drosera capensis will be triggered to close all the petals (Figure 4A-iii). At the same time, the strain and strain rate of the bending petals are monitored through the strain and piezoelectric sensors for the feedback of the real-time predation status (Figure 4B). The small-volume (solid structure) and

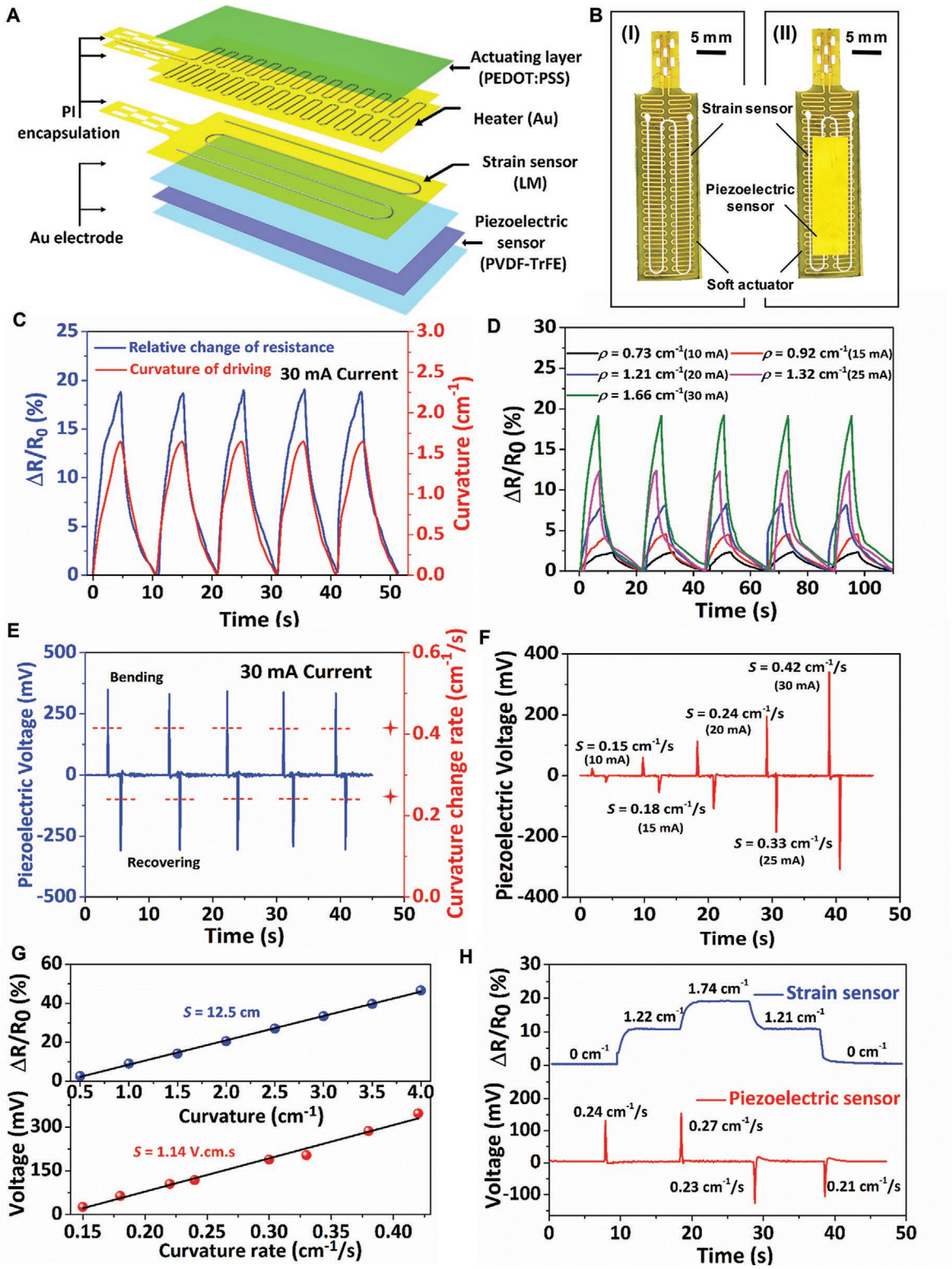

Figure 3. Bending strain and strain rate sensing demonstrations of the dual-mode sensors. A) Schematics of the soft actuator with dual-mode sensing capability by integrating an imbedded flexible heater, a strain sensor, and a piezoelectric sensor. B) Optical images of the fabricated integrated device before and after integrating the piezoelectric sensor. C) Relative resistance change of LM and E) voltage of the piezoelectric sensor with applied 30 mA current to the actuator for five cycles. D) Relative resistance change of LM and F) voltage of the piezoelectric sensor with different curvatures under applied current range from 10 to 30 mA. G) The sensitivity of the strain sensor for the curvature from 0.5 to 4 cm^{-1}, whereas the sensitivity of the piezoelectric sensor as the curvature rate of the actuator increases from 0.15 to 0.42 cm^{-1} s^{-1}. H) Measured relative resistance change and piezoelectric voltage as the actuator varies the bending curvature, rate, and direction.

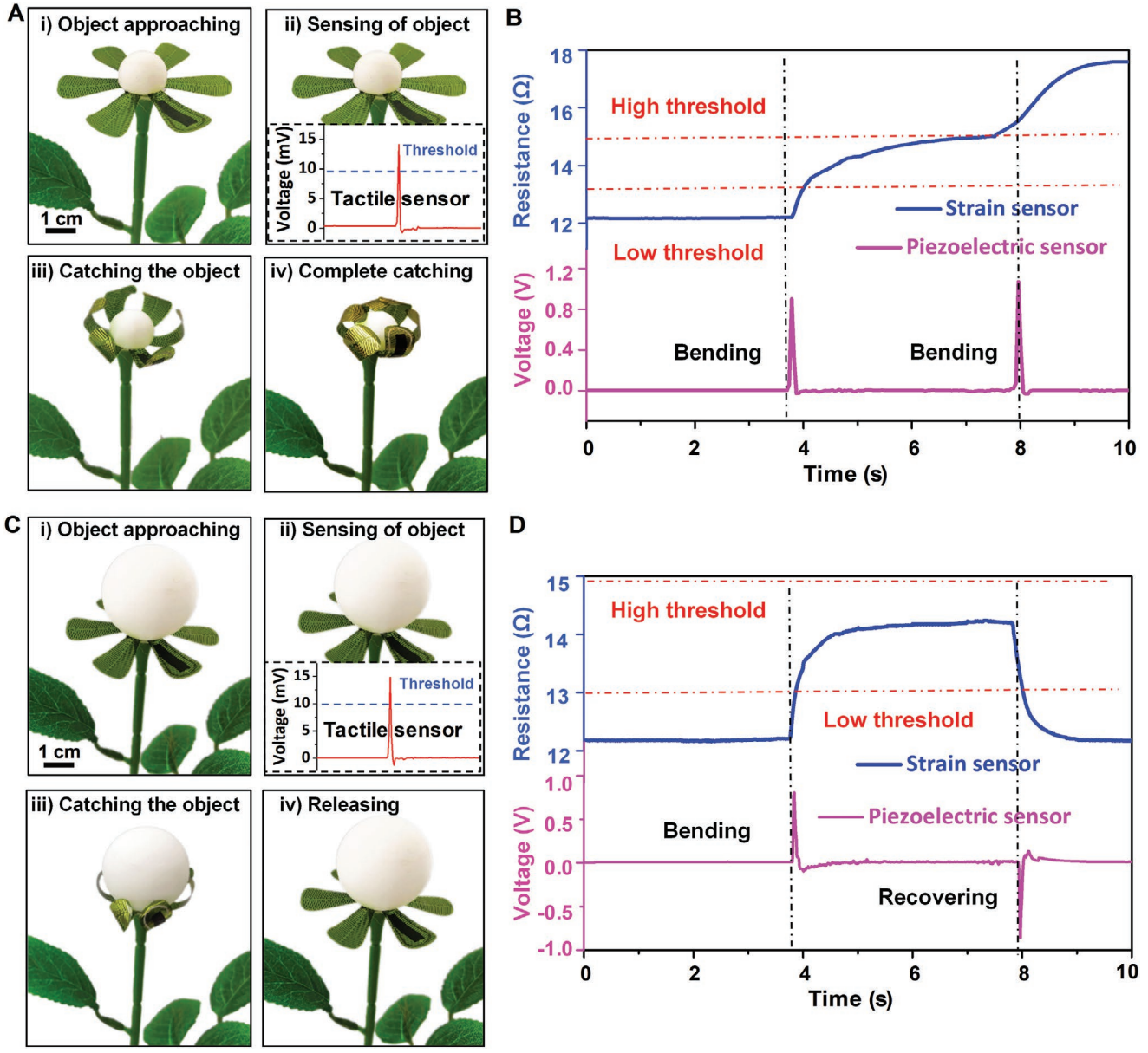

Figure 4. Demonstration of a biomimetic electronic drosera capensis with intelligent predation capability. The photo images showing the different responses of the electronic drosera capensis to small-volume preys and large-volume preys. A) For small-volume preys, the artificial drosera capensis bends twice to finish the capture of prey with a resistance level above the high threshold. C) For large-volume preys, the artificial drosera capensis does not accomplish the grasping action due to the low level of resistance of the strain sensor. Measured resistance and voltage output from the piezoelectric and strain sensor during the process of capturing B) small-volume and D) large-volume preys.

large-volume (hollow structure) objects are 3D printed with the same weight of 2.4 g to explore the effect of object size, without the effect of weight, on the autonomous actuation and adaptive predation behavior. The size of the object can be directly and quantitatively reflected by the resistance change of the strain sensor integrated in the petal. Furthermore, the preset high thresholds of the resistance value determine the size of the captured object, which is set according to the change of relative resistance caused by the half envelope state of drosera capensis. The bending strain threshold-dependent current regulation is utilized to further control the soft actuator to make an adaptive response to different stimuli. The main difference between capture and release actions lies in whether the resistance threshold is reached, which subsequently activates the electrochemical actuators to accomplish or recover the motions. Further predation actions of the electronic drosera capensis can be triggered only if the detected resistance by the strain sensor is above the high threshold (Figure 4A-iv), thus completing the process of catching small-volume preys by increasing the actuating current in an autonomous manner (Movie S2, Supporting

Information). In contrast, the resistance of the strain sensors between the low and high threshold triggers the stop action of the actuator to give up the predation of large-volume objects (Figure 4C,D). The recovery of the petals can be achieved by stopping the applied actuating current to further realize the purpose of self-protection (Movie S3, Supporting Information).

3. Conclusion

In summary, we demonstrated a unique biomimetic drosera capensis that is capable of multifunctional self-sensing, autoselect prey capture with ideal size in an entirely closed-loop fashion. An embedded flexible heater is designed to deliver joule heat to deform the thermal responsive programmable soft actuator in a highly reversible and addressable manner, whose manipulation is triggered by the perceived environmental stimuli through a tactile sensing module. Such fast predation motion (i.e., bending strain, strain rate, and bending direction) is deconvoluted by utilizing the synergistic effect between the strain and piezoelectric signals, which is further applied to induce self-regulated and feedback-type actuation. The unification of multiple self-sensing and fast actuating is beneficial to achieve the integration of sensory, neurons, and motility functionality. The developed closed-loop system with multimodal sensing using liquid alloy/P(VDF-TrFE) composites and self-regulated actuating using a special bimorph layer shows potential applications in intelligent soft robotics, human-machine interfaces, and electronic prostheses.

4. Experimental Section

Fabrication of Flexible Heaters: To prepare the flexible heaters, the PI precursor (ZKPI-305IIE, POME) was spin-coated at 1200 rpm for 60 s and cured on a hotplate at 80 °C for 30 min, 110 °C for 60 min, and 230 °C for 120 min, respectively. Then, the metal layers (Cr/Au, 10 nm/200 nm) were deposited on the PI layer by an e-Beam evaporator and followed by the lift-off process. Thereafter, another layer of PI (ZKPI-305IIE, POME) as encapsulation was spin-coated at 1200 rpm for 60 s and cured at 80 °C for 30 min, 110 °C for 60 min, and 230 °C for 120 min. The whole bilayer PI film was patterned by ICP with the deposited and patterned aluminum as the barrier layer. The flexible heaters were released from the glass substrate by immersion in BOE (1:6).

Fabrication of PI-PEDOT: PSS Actuators: The surface of PI (i.e., upper surface of the heater) was treated by an air plasma (Harrick PDC-002 Plasma Cleaner, Harrick Plasma) with a power of P = 3 W for 60 s to modify its surface with hydroxyl groups and render it hydrophilic. Next, a commercially available PEDOT: PSS aqueous dispersion (Clevios PH 1000) was deposited by spin coating at a rate of 2000 rpm for 60 s onto the plasma-treated PI substrate. After each deposition step, the samples were placed on a hot plate in ambient air for 5 min at 50 °C and air plasma treated at 3 W for 10 s to obtain 8 layers of uniform PEDOT: PSS.

Fabrication of Integrated LM Sensors: The eutectic metal alloy was synthesized by mixing gallium (75%) and indium (25%) (EGaIn, Sigma-Aldrich), which maintains a liquid state at room temperature (15.7 °C melting point). The eutectic metal alloy was stirred in the air at room temperature with 500 rpm for 2 min and 2000 rpm (vigorously stirred) for 8 min. After stirring, the LM wire was fabricated by printing it onto the substrate. After the copper wires were attached to the printed LM wire, another PI covering layer was coated on the top and cured at 250 °C for 1 h.

Preparation of P(VDF-TrFE) Piezoelectric Films: The P(VDF-TrFE) powder (Piezotech) was first mixed with N, N-Dimethylformamide (DMF) at a molar ratio of 70 to 30. Stirring the mixture at room temperature for 2 h yielded a uniform solution. Casting the uniform solution on the petri dish, followed by annealing at 120 °C for 2 h to enhance crystallinity, prepared the P(VDF-TrFE) film. After peeling off from the petri dish, the film was then polarized by placing it in a silicone oil bath at an electric field of 60 MV m^{-1} for half an hour. High piezoelectric properties were obtained in the resulting film (e.g., d_{33} = 26 pC N^{1}). The fabrication of the piezoelectric sensor started with evaporating the gold electrodes with a thickness of 150 nm on both sides of the piezoelectric film by using an electron beam evaporator (DZS-500). Attaching the copper wires to the upper and lower gold electrodes obtained the sandwich-structured piezoelectric sensors.

Measurements of the Self-Sensing Performance of the Soft Actuators: To characterize the self-sensing actuation of electrically activated soft actuators, the strain and piezoelectric signals of the sensors induced by the actuating deformation were measured by using a semiconductor parameter analyzer (4200-SCS, Keithley) and piezoelectric data acquisition system (KSI), respectively.

Supporting Information

Supporting Information is available from the Wiley Online Library or from the author.

Acknowledgements

Y.Q., C.J.W., and X.Y.L. contributed equally to this work. This work was supported by the National Natural Science Foundation of China (Grant no. 11672269, 11972323, 51572242, and 51675485); Zhejiang Provincial Natural Science Foundation of China (Grant no. LR20A020002, LR19E020004, and LR18E050002); and Fundamental Research Funds for the Provincial Universities of Zhejiang (RF-B2019004); 111 Project (No.: D16004).

Conflict of Interest

The authors declare no conflict of interest.

Data Availability Statement

Research data are not shared.

Keywords

adaptive actuation, automatic regulation, biomimetic drosera capensis, impressive predatory behavior, multifunctional self-sensing

Received: October 11, 2021
Revised: November 11, 2021
Published online:

[1] D. Rus, M. T. Tolley, *Nature* **2015**, *521*, 467.
[2] O. M. Wani, H. Zeng, A. Priimagi, *Nat. Commun.* **2017**, *8*, 15546.
[3] C. Wang, K. Sim, J. Chen, H. Kim, Z. Rao, Y. Li, W. Chen, J. Song, R. Verduzco, C. Yu, *Adv. Mater.* **2018**, *30*, 1706695.

[4] S. J. Park, M. Gazzola, K. S. Park, S. Park, V. Di Santo, E. L. Blevins, J. U. Lind, P. H. Campbell, S. Dauth, A. K. Capulli, F. S. Pasqualini, S. Ahn, A. Cho, H. Y. Yuan, B. M. Maoz, R. Vijaykumar, J. W. Choi, K. Deisseroth, G. V. Lauder, L. Mahadevan, K. K. Parker, *Science* **2016**, *353*, 158.
[5] P. Wu, J. Wang, L. Jiang, *Mater. Horiz.* **2020**, *7*, 338.
[6] Y. Naidoo, S. Heneidak, *Botany* **2013**, *91*, 234.
[7] X. Q. Wang, K. H. Chan, Y. Cheng, T. Ding, T. Li, S. Achavananthadith, S. Ahmet, J. S. Ho, G. W. Ho, *Adv. Mater.* **2020**, *32*, 2000351.
[8] M. Baumgartner, F. Hartmann, M. Drack, D. Preninger, D. Wirthl, R. Gerstmayr, L. Lehner, G. Mao, R. Pruckner, S. Demchyshyn, L. Reiter, M. Strobel, T. Stockinger, D. Schiller, S. Kimeswenger, F. Greibich, G. Buchberger, E. Bradt, S. Hild, S. Bauer, M. Kaltenbrunner, *Nat. Mater.* **2020**, *19*, 1102.
[9] Y. S. Zhao, C. Xuan, X. S. Qian, Y. Alsaid, M. T. Hua, L. H. Jin, X. M. He, *Sci. Robot.* **2019**, *4*, eaax7112.
[10] T. F. Li, G. R. Li, Y. M. Liang, T. Y. Cheng, J. Dai, X. X. Yang, B. Y. Liu, Z. D. Zeng, Z. L. Huang, Y. W. Luo, T. Xie, W. Yang, *Sci. Adv.* **2017**, *3*, e1602045.
[11] H. Shim, K. Sim, F. Ershad, P. Y. Yang, A. Thukral, Z. Rao, H. J. Kim, Y. H. Liu, X. Wang, G. Y. Gu, L. Gao, X. R. Wang, Y. Chai, C. J. Yu, *Sci. Adv.* **2019**, *5*, eaax4961.
[12] X. Yu, Z. Xie, Y. Yu, J. Lee, A. Vazquez-Guardado, H. Luan, J. Ruban, X. Ning, A. Akhtar, D. Li, B. Ji, Y. Liu, R. Sun, J. Cao, Q. Huo, Y. Zhong, C. Lee, S. Kim, P. Gutruf, C. Zhang, Y. Xue, Q. Guo, A. Chempakasseril, P. Tian, W. Lu, J. Jeong, Y. Yu, J. Cornman, C. Tan, B. Kim, K. Lee, X. Feng, Y. Huang, J. A. Rogers, *Nature* **2019**, *575*, 473.
[13] D. Yan, J. Chang, H. Zhang, J. Liu, H. Song, Z. Xue, F. Zhang, Y. Zhang, *Nat. Commun.* **2020**, *11*, 1180.
[14] J. Li, Y. Wang, L. Liu, S. Xu, Y. Liu, J. Leng, S. Cai, *Adv. Funct. Mater.* **2019**, *29*, 1903762.
[15] Y. Ling, W. Pang, X. Li, S. Goswami, Z. Xu, D. Stroman, Y. Liu, Q. Fei, Y. Xu, G. Zhao, B. Sun, J. Xie, G. Huang, Y. Zhang, Z. Yan, *Adv. Mater.* **2020**, *32*, 1908475;
[16] K. Sim, Z. L. Rao, Z. N. Zou, F. Ershad, J. M. Lei, A. Thukral, J. Chen, Q. A. Huang, J. L. Xiao, C. J. Yu, *Sci. Adv.* **2019**, *5*, eaav9653.
[17] L. Tian, B. Zimmerman, A. Akhtar, K. J. Yu, M. Moore, J. Wu, R. J. Larsen, J. W. Lee, J. Li, Y. Liu, B. Metzger, S. Qu, X. Guo, K. E. Mathewson, J. A. Fan, J. Cornman, M. Fatina, Z. Xie, Y. Ma, J. Zhang, Y. Zhang, F. Dolcos, M. Fabiani, G. Gratton, T. Bretl, L. J. Hargrove, P. V. Braun, Y. Huang, J. A. Rogers, *Nat. Biomed. Eng.* **2019**, *3*, 194.
[18] J. Kim, M. Lee, H. J. Shim, R. Ghaffari, H. R. Cho, D. Son, Y. H. Jung, M. Soh, C. Choi, S. Jung, K. Chu, D. Jeon, S. T. Lee, J. H. Kim, S. H. Choi, T. Hyeon, D. H. Kim, *Nat. Commun.* **2014**, *5*, 5747.
[19] Y. Kim, H. Yuk, R. Zhao, S. A. Chester, X. Zhao, *Nature* **2018**, *558*, 274.
[20] Y. Kim, G. A. Parada, S. D. Liu, X. H. Zhao, *Sci. Robot.* **2019**, *4*, eaax7329.
[21] S. Y. Zhuo, Z. G. Zhao, Z. X. Xie, Y. F. Hao, Y. C. Xu, T. Y. Zhao, H. J. Li, E. L. Knubben, L. Wen, L. Jiang, M. J. Liu, *Sci. Adv.* **2020**, *6*, eaax1464.
[22] C. H. Linghu, S. Zhang, C. J. Wang, K. X. Yu, C. L. Li, Y. J. Zeng, H. D. Zhu, X. H. Jin, Z. Y. You, J. Z. Song, *Sci. Adv.* **2020**, *6*, eaay5120.
[23] Y. Y. Xiao, Z. C. Jiang, X. Tong, Y. Zhao, *Adv. Mater.* **2019**, *31*, 1903452.
[24] H. Lu, Y. Hong, Y. Yang, Z. Yang, Y. Shen, *Adv. Sci.* **2020**, *7*, 2000069.
[25] L. Chen, M. Weng, P. Zhou, F. Huang, C. Liu, S. Fan, W. Zhang, *Adv. Funct. Mater.* **2019**, *29*, 1806057.
[26] Y. C. Lai, J. Deng, R. Liu, Y. C. Hsiao, S. L. Zhang, W. Peng, H. M. Wu, X. Wang, Z. L. Wang, *Adv. Mater.* **2018**, *30*, 1801114.
[27] M. Amjadi, M. Sitti, *Adv. Sci.* **2018**, *5*, 1800239.
[28] D. Chen, Q. Liu, Z. Han, J. Zhang, H. Song, K. Wang, Z. Song, S. Wen, Y. Zhou, C. Yan, Y. Shi, *Adv. Sci.* **2020**, *7*, 2000584.
[29] K. He, Y. Liu, M. Wang, G. Chen, Y. Jiang, J. Yu, C. Wan, D. Qi, M. Xiao, W. R. Leow, H. Yang, M. Antonietti, X. Chen, *Adv. Mater.* **2020**, *32*, 1905399.
[30] Y. Lee, J. Y. Oh, W. Xu, O. Kim, T. R. Kim, J. Kang, Y. Kim, D. Son, J. B. H. Tok, M. J. Park, Z. N. Bao, T. W. Lee, *Sci. Adv.* **2018**, *4*, eaat7387.
[31] C. Larson, B. Peele, S. Li, S. Robinson, M. Totaro, L. Beccai, B. Mazzolai, R. Shepherd, *Science* **2016**, *351*, 1071.
[32] M. Kanik, S. Orguc, G. Varnavides, J. Kim, T. Benavides, D. Gonzalez, T. Akintilo, C. C. Tasan, A. P. Chandrakasan, Y. Fink, P. Anikeeva, *Science* **2019**, *365*, 145.
[33] A. Fleischmann, P. M. Gonella, *Taxon* **2020**, *69*, 153.
[34] M. Krausko, Z. Perutka, M. Sebela, O. Samajova, J. Samaj, O. Novak, A. Pavlovic, *New Phytol.* **2017**, *213*, 1818.
[35] C. A. M. La Porta, M. C. Lionetti, S. Bonfanti, S. Milan, C. Ferrario, D. Rayneau-Kirkhope, M. Beretta, M. Hanifpour, U. Fascio, M. Ascagni, L. De Paola, Z. Budrikis, M. Schiavoni, E. Falletta, A. Caselli, O. Chepizhko, A. Tuissi, A. Vailati, S. Zapperi, *Proc. Natl. Acad. Sci. USA* **2019**, *116*, 18777.
[36] S. Taccola, F. Greco, E. Sinibaldi, A. Mondini, B. Mazzolai, V. Mattoli, *Adv. Mater.* **2015**, *27*, 1668.
[37] Y. Cui, C. Wang, K. Sim, J. Chen, Y. Li, Y. Xing, C. Yu, J. Song, *AIP Adv.* **2018**, *8*, 025215.
[38] H. Deng, C. Zhang, J. W. Su, Y. Xie, C. Zhang, J. Lin, *J. Mater. Chem. B* **2018**, *6*, 5415.
[39] S. Yao, J. Cui, Z. Cui, Y. Zhu, *Nanoscale* **2017**, *9*, 3797.
[40] J. K. Mu, C. Y. Hou, H. Z. Wang, Y. G. Li, Q. H. Zhang, M. F. Zhu, *Sci. Adv.* **2015**, *1*, e1500533.
[41] L. Chen, M. Weng, W. Zhang, Z. Zhou, Y. Zhou, D. Xia, J. Li, Z. Huang, C. Liu, S. Fan, *Nanoscale* **2016**, *8*, 6877.
[42] T. Wang, M. Li, H. Zhang, Y. Sun, B. Dong, *J. Mater. Chem. C* **2018**, *6*, 6416.
[43] M. D. Dickey, *Adv. Mater.* **2017**, *29*, 1606425.
[44] N. Kazem, T. Hellebrekers, C. Majidi, *Adv. Mater.* **2017**, *29*, 1605985.
[45] Y. R. Jeong, J. Kim, Z. Xie, Y. Xue, S. M. Won, G. Lee, S. W. Jin, S. Y. Hong, X. Feng, Y. Huang, J. A. Rogers, J. S. Ha, *NPG Asia Mater.* **2017**, *9*, e443.
[46] Y. Qiu, Y. Tian, S. Sun, J. Hu, Y. Wang, Z. Zhang, A. Liu, H. Cheng, W. Gao, W. Zhang, H. Chai, H. Wu, *Nano Energy* **2020**, *78*, 105337.